

## Characterization of the intrinsic density profiles for liquid surfaces

This article has been downloaded from IOPscience. Please scroll down to see the full text article.

2005 J. Phys.: Condens. Matter 17 S3493

(<http://iopscience.iop.org/0953-8984/17/45/039>)

View [the table of contents for this issue](#), or go to the [journal homepage](#) for more

Download details:

IP Address: 129.252.86.83

The article was downloaded on 28/05/2010 at 06:42

Please note that [terms and conditions apply](#).

# Characterization of the intrinsic density profiles for liquid surfaces

Enrique Chacón<sup>1</sup> and Pedro Tarazona<sup>2</sup>

<sup>1</sup> Instituto de Ciencia de Materiales de Madrid, Consejo Superior de Investigaciones Científicas, Madrid 28049, Spain

<sup>2</sup> Departamento de Física Teórica de la Materia Condensada, Universidad Autónoma de Madrid, 28049 Madrid, Spain

E-mail: [echacon@icmm.csic.es](mailto:echacon@icmm.csic.es) and [pedro.tarazona@uam.es](mailto:pedro.tarazona@uam.es)

Received 16 September 2005

Published 28 October 2005

Online at [stacks.iop.org/JPhysCM/17/S3493](http://stacks.iop.org/JPhysCM/17/S3493)

## Abstract

This paper presents recent advances in the characterization of the intrinsic structures in computer simulations of liquid surfaces. The use of operational definitions for the intrinsic surface, associated with each molecular configuration of a liquid slab, gives direct access to the intrinsic profile and to the wavevector dependent surface tension. However, the characteristics of these functions depend on the definition used for the intrinsic surface. We discuss the pathologies associated with a local Gibbs dividing surface definition, and consider the alternative definition of a minimal area surface, going through a set of surface pivots, self-consistently chosen to represent the first liquid layer.

The classical capillary wave theory (CWT) [1, 2] assumes the existence of an *intrinsic profile* which describes the structure of the liquid surface without the blurring effect of the capillary wave (CW) fluctuations. There is an undetermined upper wavelength cut-off  $q_u$ , used to separate the low- $q$  *surface* fluctuations from those typical of the *bulk* liquid [3]; and the choice of  $q_u$  should affect the shape of the intrinsic profile  $\tilde{\rho}(z, q_u)$ . Within the CWT hypothesis, the *mean* density profile, averaged over a transverse area  $A \equiv L^2$ , is the convolution of  $\tilde{\rho}(z, q_u)$  with a Gaussian of squared width  $\Delta(L, q_u)$ , which adds the fluctuations of the *intrinsic surface* for wavevector values  $2\pi/L \leq q \leq q_u$ . The validity of the CWT is well established for  $q_u\sigma \ll 1$ , in terms of the molecular diameter  $\sigma$ ; however, the increasing accuracy of the x-ray surface diffraction measurements [4–6] has pushed towards the use of the CWT to interpret the experimental data up to atomic resolution, and to extend the theory with the use of a wavevector dependent surface tension  $\gamma(q)$  [7], which reduces to the macroscopic value  $\gamma_0$  for  $q\sigma \ll 1$ . If, with growing  $q$ ,  $\gamma(q)$  becomes much larger than  $\gamma_0$ , then the CW spectrum would die smoothly at large  $q$ , instead of having a sharp cut-off; and there would be a *sharpest* intrinsic representation of the surface in which the *full* CW spectrum allowed by the system size would be extracted. The x-ray reflectivity data for cold liquid metal surfaces [5, 6] were interpreted in these terms, with a delta function to represent the *first liquid layer* in the intrinsic

profiles, and a cut-off  $q_u \approx \pi/\sigma$  in the classical CWT, which should be interpreted [4] as the effective sharp cut-off providing the same value of  $\Delta(L, q_u)$  (with constant  $\gamma_0$ ) as the *total* CW fluctuation (with  $\gamma(q)$ ) for all  $q \geq 2\pi/L$ .

Computer simulations of liquid slabs may be used to test the validity of that interpretation, with any operational definition of the instantaneous intrinsic surface,  $\xi(\mathbf{R}) = \sum_q \hat{\xi}_q \exp(i\mathbf{q} \cdot \mathbf{R})$ , to be associated with the molecular positions  $\mathbf{r}_i \equiv (\mathbf{R}_i, z_i)$ , for  $i = 1$  to  $N$ . The intrinsic density profile may be obtained as the statistical average

$$\tilde{\rho}(z) = \frac{1}{A} \left\langle \sum_i \delta(z - z_i + \xi(\mathbf{R}_i)) \right\rangle, \quad (1)$$

and the mean squared amplitude  $\langle |\hat{\xi}_q|^2 \rangle$  gives directly the function

$$\gamma(q) = \frac{kT}{q^2 \langle |\hat{\xi}_q|^2 \rangle A}. \quad (2)$$

Both  $\tilde{\rho}(z)$  and  $\gamma(q)$  would depend on the particular definition of the intrinsic surface associated with each molecular configuration; different choices for  $\xi(\mathbf{R})$  would reproduce the same CW spectrum for  $q\sigma \ll 1$ , but when the description is pushed to the range  $q\sigma \approx 1$  the fluctuation spectrum of  $\xi(\mathbf{R})$  becomes strongly entangled with its definition.

The simplest definition of  $\xi(\mathbf{R})$  is a local version of the Gibbs dividing surface, applied over prisms of transverse length  $\sim 2\pi/q_u$ , which has been used to evaluate  $\gamma(q)$  in several models [8, 9], always in good agreement with the CWT assumption  $\gamma(q) \approx \gamma_0$  for small  $q$ , but with the puzzling result of being a decreasing (rather than increasing) function of  $q$ , so that the squared CW amplitude grows with  $q$ , without a natural upper cut-off for the CW spectrum. This is produced by the failure in the separation of *surface* and *bulk* fluctuations, with that definition of  $\xi(\mathbf{R})$ ; so that for  $q > \pi/\sigma$  the putative mean squared amplitude  $\langle |\hat{\xi}_q|^2 \rangle$  becomes proportional to the bulk structure factor of the liquid [10], rather than to the fluctuations of the local position of the interface. The intrinsic profiles  $\tilde{\rho}(z, q_u)$  evaluated with this  $\xi(\mathbf{R})$  give the expected sharpening of the surface structure, with respect to the mean profile  $\rho(z, L)$  for  $2\pi/L < q_u < \sigma^{-1}$ , but when the upper cut-off is pushed behind that limit  $\tilde{\rho}(z, q_u)$  becomes smoother, instead of sharper [12].

In recent works [11, 12] we have explored an alternative definition, which links  $\xi(\mathbf{R})$  directly to a set of *pivot molecules* on the liquid surface, instead of relying on a density balance across the interface. The intrinsic surface is defined as the *minimal area* surface, with an upper Fourier component cut-off  $q_{\max} \approx 2\pi/\sigma$ , and going through a set of *surface pivots*. The key point is a procedure to select those pivots at the most external molecules of the liquid slab, segregated from those in the vapour by a simple percolation algorithm. In our test for simple atomic liquids [11, 12], we start with a small initial set of surface pivots, and a very flat minimal surface  $\xi(\mathbf{R})$ ; then we use a parameter  $\tau \approx 0.5\sigma$  to incorporate new pivots at those atoms on the liquid surface separated from  $\xi(\mathbf{R})$  by a distance less than  $\tau$ ; a rougher intrinsic surface is then recalculated with the enlarged set of pivots, and the process is iterated until there were no atoms with  $|\xi(\mathbf{R}_i) - z_i| \leq \tau$  in the sample. The results for  $\tilde{\rho}(z, q_{\max})$  and  $\gamma(q)$  obtained with this method, for several simple fluid models with pairwise isotropic interactions, were discussed in our previous works [11, 12]; the dependence on the parameter  $\tau$  is very sharp, with an upper threshold,  $\tau_{\text{thr}}$ , beyond which the number of surface pivots does not converge, and  $\xi(\mathbf{R})$  becomes a meaningless rough surface cutting across the liquid slab. Values of  $\tau$  much lower than  $\tau_{\text{thr}}$  produce unphysical shapes for the intrinsic profiles, while those within a small range of  $\tau < \tau_{\text{thr}}$  have an aspect qualitatively similar to the intrinsic profiles extracted from x-ray reflectometry for cold liquid metals [5, 6]. The number of pivot atoms per unit area gives the two-dimensional density  $n_0$ , associated with the delta-function in  $\tilde{\rho}(z, q_{\max})$ , to

represent the *first liquid layer*, followed by an oscillatory structure qualitatively similar to that of the pair distribution function of the bulk liquid. This is the sharpest intrinsic view of the interface, similar to that used in the interpretation of the x-ray reflectivity data, and described as a *distorted solid* [5] with a sum of Gaussian layers of increasing width, to represent the accumulation of fluctuations with respect to the nominal position of the layer, as the layer index goes into the liquid bulk. Our computer simulations established the existence of strong correlations between  $\tilde{\rho}(z, q_{\max})$  and  $\xi(\mathbf{R})$ , which go beyond the CWT hypothesis [12], but they may be systematically reduced with a less sharp representation of the surface, restricting the shape of  $\xi(\mathbf{R})$  to Fourier components  $q \leq q_u < q_{\max}$ . The function  $\gamma(q)$  obtained with our definition also depends on  $\tau$ , and for the choice of this parameter leading to the best shape for  $\tilde{\rho}(z, q_{\max})$  the function  $\gamma(q)$  goes rather flat to the macroscopic surface tension  $\gamma_0$  at low  $q$  and increases rapidly as  $q$  approaches  $2\pi/\sigma$ , so that the CW spectrum ends smoothly as we approach the molecular limit for the corrugations of the intrinsic surface.

Although the results for  $\tilde{\rho}(z, q_u)$ , with several simple fluid models, are qualitatively satisfactory [11, 12], the use of  $\tau$  as a control parameter for the definition of  $\xi(\mathbf{R})$  presents some problems. The self-consistent addition of new pivots has to separate the *first* from the *inner liquid layers*, and obviously these are *soft* concepts for which we cannot expect a sharp separation. The physical picture of the liquid surface given by our  $\tilde{\rho}(z, q_{\max})$  is a clear local layering structure, but with stronger in-layer fluctuations as  $T$  increases. The choice of  $\tau$ , or any other specification in the definition of  $\xi(\mathbf{R})$ , gives an (arbitrary) discrimination between what is considered an inwards CW fluctuation, of the *first* liquid layer, and what is considered an outwards fluctuation within the *second* liquid layer. The latter would contribute to the finite width of the inner layer in  $\tilde{\rho}(z, q_{\max})$ , while the former is ironed out in (1). Setting a minimum distance,  $\tau$ , from any of these *second layer* fluctuations to the intrinsic surface, and in any sampled configuration, should produce a (sample and system) size dependence of the upper threshold  $\tau_{\text{thr}}$ , as in any percolation problem. In our application of the method to cold liquid surfaces (with  $T/T_C < 0.3$ ), and with total sampled areas up to  $10^6\sigma^2$ , that size dependence was well below our accuracy for the determination of  $\tau_{\text{thr}}$ , and hence irrelevant for practical purposes. However, at higher temperatures the value of  $\tau_{\text{thr}}$  was pushed down by a just small number of configurations, and larger samples would push it to still lower values, while most configurations would be better described by the intrinsic profiles with  $\tau > \tau_{\text{thr}}$ . The problem becomes much more important when the method is applied to anisotropic molecular fluids [13] since the layering defects are strongly enhanced by the disorder in the molecular orientations.

An alternative procedure explored here is to use the *first layer density*  $n_0$  as control parameter, so that we describe all the configurations with exactly the same number of pivot molecules, which are selected by self-consistent addition (one by one, or in small batches) of those molecules which are closer to the minimal surface which goes through all the previously selected pivots. The procedure is computationally more costly than the previous one, since it requires more evaluations of the minimal surfaces, but still we may perform the calculations for similar sample sizes as used before. For each configuration the minimum distance of a non-pivot molecule to the final  $\xi(\mathbf{R})$  (calculated with exactly  $n_0 A$  pivots), corresponds to the value of the parameter  $\tau$  in the previous definition; the average over configurations gives  $\langle \tau \rangle \pm \Delta\tau$ , as a function of the control parameter  $n_0$ ; equivalently to the results  $\langle n_0 \rangle \pm \Delta n_0$ , for a fixed value of  $\tau$ , with the other method. The qualitative difference is that increasing  $n_0$  gives always smooth variations of  $\langle \tau \rangle$ , while the increase of  $\tau$  beyond  $\tau_{\text{thr}}$  produces a sudden increase of  $\langle n_0 \rangle$ . At low temperature, the existence of such a threshold helped to fix a small range of reasonable values for the parameter  $\tau$  for an isotropic and cold liquid surface.

In figure 1(a) we present the intrinsic profiles for a very cold liquid surface,  $T/T_C \approx 0.12$ , near the triple point of a simple fluid with very soft core repulsion, the soft-alkali model of [14].

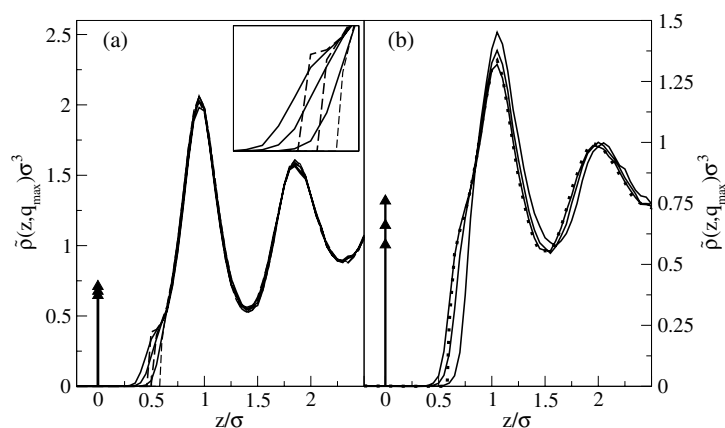


**Figure 1.** Intrinsic profiles at the sharpest resolution,  $\tilde{\rho}(z, q_{\max})$ , in atomic diameter units,  $\sigma$ . Left panel: results for the soft-alkali model at  $T/T_C \approx 0.12$ ; the broken lines are obtained with our previous method and three values of  $\tau\sigma$  (0.46, 0.52 and 0.58). The present method gives the full lines when the first layer density is set equal to its previous mean values ( $\langle n_0 \rangle \sigma^2 = 0.69, 0.72$  and  $0.75$ ). Right panel: results for the Lennard-Jones fluid at  $T/T_C \approx 0.56$ . The dotted line gives the result with our previous method at the threshold value  $\tau\sigma \approx 0.58$ . The full lines show the results of the present method for  $n_0\sigma^2 = 0.62$  (equal to the previous  $\langle n_0 \rangle$ ) and two higher values, 0.7 and 0.8. In both panels the arrows show the first layer ( $\delta$ -function) density.

The dashed lines give the results of our previous method, with three different values of  $\tau$ ; while the full lines give the results with fixed values of  $n_0$ , set to be exactly the mean values  $\langle n_0 \rangle$  with the fixed  $\tau$  procedure. The results show that (for reasonable values for the parameters) the intrinsic profiles differ only in the small region (inset) with  $z \approx \tau \approx \sigma/2$ , where the sharp step produced with a fixed  $\tau$  becomes now a more appealing smooth decay for fixed  $n_0$ . The best choice for  $n_0$  may be done in the same terms as for  $\tau$  before, looking for the best Gaussian fit of the second peak in  $\tilde{\rho}(z, q_{\max})$ , and simultaneously for the best Gaussian fit of the first layer for  $q_u < q_{\max}$ . Too low values of  $n_0$  are discarded by the presence of a shoulder in  $\tilde{\rho}(z, q_{\max})$  at  $z \approx 0.5$ , formed by the molecules which should have been naturally assigned to the first layer rather than to the second one; on the other hand, too large values of  $n_0$  are identified by the non-Gaussian structure of the first peak in  $\tilde{\rho}(z, q_u)$ , when  $q_u$  is reduced below its maximum value used for the selection of pivots. At the low temperature of the results in figure 1(a) we obtain similar values for the best fitting  $n_0$  and for the best fitting  $\tau$ , although the quality of the Gaussian fits is clearly improved with the new method, since the sharp cut-off of  $\tilde{\rho}(z, q_{\max})$  at  $z = \tau$  is eliminated.

However, when the in-layer fluctuations become stronger, at the typical temperatures of simple liquids, the value of  $\tau_{\text{thr}}$  was lowered by a few configurations, well below what would be the optimal value to get the best Gaussian fit in all the others. With the new method we may explore values of  $n_0$  well above that of  $\langle n_0 \rangle$  at  $\tau = \tau_{\text{thr}}$ , and improve the shape of the second peak in  $\tilde{\rho}(z, q_{\max})$ . This is clear in figure 1(b), for the Lennard-Jones fluid at  $T/T_C = 0.56$ , near its triple point; the dotted line corresponds to our previous results, with  $\tau_{\text{thr}} \approx 0.56\sigma$ ; and the broken line in that figure gives the result with our new method, when the number of pivots is set to take exactly the mean value  $\langle n_0 \rangle = 0.62\sigma^{-2}$  obtained for that  $\tau_{\text{thr}}$ . However, increasing that value up to  $n_0 = 0.8\sigma^{-2}$  gives the intrinsic profile represented by the full lines, with a clearly more natural (Gaussian) shape for the layer around  $z = \sigma$ , and a slight shift in the inner layer structure. That confirms, and somewhat improves, our previous claim of a strong surface layering structure as a generic property of liquid interfaces, and not restricted to cold liquid

metals. The smooth density profiles of the LJ liquid, when averaged over the typical transverse sizes ( $L \sim 10\sigma$ ) of computer simulations, hide intrinsic profiles with a structure qualitatively similar to that of the liquid pair distribution function  $g(r)$ . The only peculiarity of the cold surfaces in liquid Hg or Ga is that the higher values of  $\gamma_0$  keep that oscillatory structure in  $\rho(z, L)$ , up to transverse sizes  $L > 300\sigma$ , within the range of experimental observation with the strongly collimated x-ray beams of the synchrotron sources.

Besides giving a slightly stronger, and somewhat better, representation of the layering structures at high  $T$ , the use of  $n_0$  as control parameter makes clear that the *best* representation of the intrinsic surface is more ambiguous than with the sharper (but less natural) choice of  $\tau_{\text{thr}}$ . The best Gaussian fits to the intrinsic profiles cannot discern between the range  $0.7$  and  $0.8\sigma^{-2}$  for the first layer density  $n_0$ , clearly above the previous estimation, but also with a larger error bar, as an intrinsic limit for determination of that quantity. Our previous claims [12] of strong temperature and model dependences of  $n_0$ , which could be taken as an intrinsic characteristics of the liquid surfaces, have to be discarded as an artifact of the lowering of  $\tau_{\text{thr}}$  by the stronger in-layer fluctuations at high temperatures. The present estimation is  $n_0 \approx 0.75 \pm 0.05\sigma^{-2}$ , apparently similar for the different simple fluid models analysed in our previous works. This suggests a generic intrinsic structure, which describes, within the unavoidable ambiguity in  $n_0$ , the surface of any simple liquid with isotropic pair interactions, and which is probably determined more by simple packing constraints than by the particular form of the interaction potential. However, larger differences may appear between the surface intrinsic structures of anisotropic molecular fluids or liquid metals.

The  $q$ -dependent surface tension  $\gamma(q)$ , obtained from (2), depends also on the choice of  $n_0$ ; hence it shares some ambiguity on what is the most natural choice, and it is important to realize that such ambiguity is intrinsic to the concept of surface tension for curved interfaces. Definitions like the local Gibbs dividing surface, which work well in the limit  $\gamma(q) \rightarrow \gamma_0$  for  $q\sigma \ll 1$ , may produce unphysical values of  $\gamma(q)$  for  $q\sigma \geq 1$ , for the same reason that they produce qualitatively wrong shapes for  $\tilde{\rho}(z, q_u)$ , i.e. because the so defined intrinsic surfaces fail to describe the local position of the interface at that molecular resolution. On the other hand, the intrinsic surfaces obtained with our method, for say  $n_0 = 0.7$  or  $0.8\sigma^{-2}$ , give both a reasonable representation of that local surface and lead to qualitatively similar, but quantitatively different, functions  $\gamma(q)$ , represented in figure 2(a), for the soft-alkali model at  $T/T_C = 0.33$ . The lower value of  $n_0$  gives flatter intrinsic surfaces, and hence higher effective surface tensions, while the rougher  $\xi(\mathbf{R})$ , going through a larger number of surface pivots, corresponds to lower values of  $\gamma(q)$ . The vertical arrows give the corresponding values of the effective upper cut-off, to reproduce within the classical CWT the mean square CW amplitude. In figure 2(b) we represent the values of that effective upper cut-off, as functions of  $n_0$ , for different temperatures and model interactions. The values of  $n_0$  compatible with qualitative good shapes of the intrinsic profiles  $\tilde{\rho}(z, q_u)$  are included in the shadowed region, which leaves a clear decay of  $q_u^{\text{eff}}$  with increasing  $T$ , from values  $q_u^{\text{eff}} \approx \pi/\sigma$ , which are typically chosen in the analysis of the experimental data [4], to about half that value at the triple point of the LJ model.

The main conclusion of this work could be that a good operational definition of intrinsic surface, to be used in computer simulations, is important to obtain an intrinsic representation of free liquid surfaces, beyond the blurring effects of the CW fluctuations. The local Gibbs dividing surface definition cannot be pushed down to the molecular scale,  $q\sigma \approx 1$ ; but other choices, more directly tied to the local position of the surface, may be successfully used to obtain the intrinsic profile and the effective surface tension  $\gamma(q)$ , with the correct qualitative features. Nevertheless, we have to make clear that (particularly at high temperatures) the details of the definition still matter for the quantitative analysis of the results; and that there is

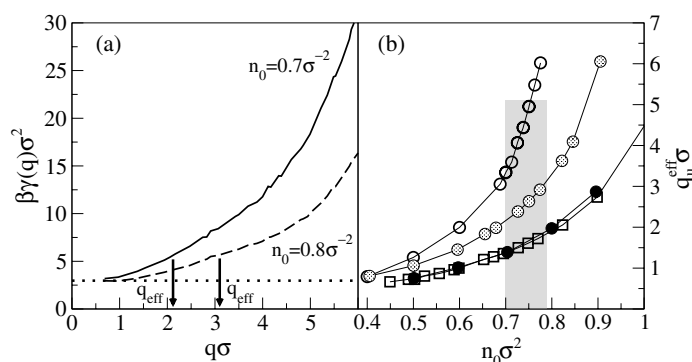


**Figure 2.** Left panel: the  $q$ -dependent surface tension  $\gamma(q)$ , in  $\beta = (k_B T)^{-1}$  and atomic diameter  $\sigma$  units, for the soft-alkali model at  $T/T_C = 0.12$ . The full line is the result with a first layer density  $n_0\sigma^2 = 0.7$  and the dashed line with  $n_0\sigma^2 = 0.8$ . The arrows indicate the corresponding values of the CWT effective upper cut-off  $q_{\text{u}}^{\text{eff}}$ . The dotted line shows the macroscopic value of the surface tension  $\gamma_0$ . Right panel: the CWT effective upper cut-off  $q_{\text{u}}^{\text{eff}}$  versus the first layer density  $n_0\sigma^2$ . The circles are the results for the soft-alkali model at  $T/T_C = 0.12$  (empty),  $T/T_C = 0.33$  (grey), and  $T/T_C = 0.65$  (black). The squares are for the Lennard-Jones model at  $T/T_C = 0.56$ . The shadowed region covers the values of  $n_0$  with a good shape for the intrinsic profiles.

no hope of a *unique* definition of  $\xi(\mathbf{R})$  which could correspond to the *true* intrinsic structure of the surface. There are more or less useful definitions which do achieve, in a better or worse way, the separation of the CW fluctuation spectrum from the bulk liquid correlation structure. Moreover, we have to be aware of the lack of statistical independence between  $\xi(\mathbf{R})$  and  $\tilde{\rho}(z, q_{\text{u}})$  when the intrinsic surface description is pushed down to the molecular scale [12], which would require a reformulated CWT theory to interpret the increasingly accurate experimental results from x-ray reflectometry.

### Acknowledgment

We acknowledge financial support by the Dirección General de Investigación of Spain under grant number FIS2004-05035.

### References

- [1] Buff F P, Lovett R A and Stinger F H 1965 *Phys. Rev. Lett.* **15** 621
- [2] Percus J R 1986 *Fluid Interfacial Phenomena* ed C A Croxton (New York: Wiley) pp 1–44
- [3] Dietrich S 1996 *J. Phys.: Condens. Matter* **8** 9127
- [4] Pershan P S 2000 *Colloids Surf. A* **171** 149
- [5] Magnussen O, Ocko B M, Regan M J, Penanen K, Pershan P S and Deutsch M 1995 *Phys. Rev. Lett.* **74** 4444
- [6] DiMasi E, Tostmann H, Ocko B M, Pershan P S and Deutsch M 1998 *Phys. Rev. B* **58** R13419
- [7] Regan M J, Kawamoto E H, Lee S, Pershan P S, Maskil N, Deutsch M, Magnussen O M, Ocko B M and Berman L E 1995 *Phys. Rev. Lett.* **75** 2498
- [8] Daillant J and Alba M 2000 *Rep. Prog. Phys.* **63** 1725
- [9] Stecki J 1998 *J. Chem. Phys.* **109** 5002
- [10] Robledo A, Varea C and Romero-Ronchin V 1991 *Physica A* **177** 474
- [11] Werner A, Schmid E, Müller M and Binder K 1997 *J. Chem. Phys.* **107** 8175
- [12] Werner A, Schmid E, Müller M and Binder K 1999 *Phys. Rev. E* **59** 728
- [13] Vink R L C, Horbach J and Binder K 2005 *J. Chem. Phys.* **122** 134905
- [14] Chacón E and Tarazona P 2003 *Phys. Rev. Lett.* **91** 166103
- [15] Tarazona P and Chacón E 2004 *Phys. Rev. B* **70** 235407
- [16] Chacón E, Tarazona P and Alejandre J 2005 at press
- [17] Chacón E, Reinaldo-Falagan M, Velasco E and Tarazona P 2001 *Phys. Rev. Lett.* **87** 166101
- [18] Velasco E, Tarazona P, Reinaldo-Falagan M and Chacón E 2002 *J. Chem. Phys.* **117** 10777